

1 **The impact of high frequency rapid viral antigen screening on COVID-19 spread**  
2 **and outcomes: a validation and modeling study**

3  
4 Authors: Beatrice Nash<sup>1,2\*</sup>, Anthony Badea<sup>1,3\*</sup>, Ankita Reddy<sup>1,4\*</sup>, Miguel Bosch<sup>1,5</sup>, Nol  
5 Salcedo<sup>1</sup>, Adam R. Gomez<sup>1</sup>, Alice Versiani<sup>6</sup>, Gislaine Celestino Dutra Silva<sup>6</sup>, Thayza  
6 Maria Izabel Lopes dos Santos<sup>6</sup>, Bruno H. G. A. Milhim<sup>6</sup>, Marilia M. Moraes<sup>6</sup>, Guilherme  
7 Rodrigues Fernandes Campos<sup>6</sup>, Flávia Quieroz<sup>6</sup>, Andreia Francesli Negri Reis<sup>6</sup>, Mauricio  
8 L. Nogueira<sup>6</sup>, Elena N. Naumova<sup>7</sup>, Irene Bosch<sup>1,8</sup>, Bobby Brooke Herrera<sup>1,9‡</sup>

9  
10 \*These authors contributed equally to this work.

11  
12 Affiliations:

13 <sup>1</sup>E25Bio, Inc., Cambridge, MA, USA

14 <sup>2</sup>Department of Computer Science, Harvard University School of Engineering and Applied  
15 Sciences, Cambridge, MA, USA

16 <sup>3</sup>Department of Physics, Harvard University, Cambridge, MA, USA

17 <sup>4</sup>Perelman School of Medicine, University of Pennsylvania, Philadelphia, PA, USA

18 <sup>5</sup>InfoGeosciences LLC, Houston, TX, USA

19 <sup>6</sup>Faculdade de Medicina de São José do Rio Preto (FAMERP), São José do Rio Preto,  
20 Brazil

21 <sup>7</sup>Division of the Nutrition Epidemiology and Data Science, Friedman School of Nutrition  
22 Science and Policy, Tufts University, Boston, MA, USA

23 <sup>8</sup>Department of Medicine, Mount Sinai School of Medicine, New York, NY, USA

24 <sup>9</sup>Department of Immunology and Infectious Diseases, Harvard T.H. Chan School of Public  
25 Health, Boston, MA, USA

26

27 ‡Corresponding Author. BBH, email: [bbherrera@e25bio.com](mailto:bbherrera@e25bio.com)

28

29

30

31

32

33

34

35

36

37

38

39

40

41

42

43

44

45

46

47 **Abstract**

48 High frequency screening of populations has been proposed as a strategy in  
49 facilitating control of the COVID-19 pandemic. Here we use computational modeling,  
50 coupled with clinical data from a rapid antigen test, to predict the impact of frequent rapid  
51 testing on COVID-19 spread and outcomes. Using patient nasopharyngeal swab  
52 specimens, we demonstrate that the sensitivity and specificity of the rapid antigen test  
53 compared to quantitative real-time polymerase chain reaction (qRT-PCR) are 84.7% and  
54 85.7%, respectively; moreover, sensitivity correlates directly with viral load. Based on  
55 COVID-19 data from three regions in the United States and São José do Rio Preto, Brazil,  
56 we show that high frequency, strategic population-wide rapid testing, even at varied  
57 accuracy levels, diminishes COVID-19 infections, hospitalizations, and deaths at a  
58 fraction of the cost of nucleic acid detection via qRT-PCR. We propose large-scale  
59 antigen-based surveillance as a viable strategy to control SARS-CoV-2 spread and to  
60 enable societal re-opening.

61

62

63

64

65

66

67

68

69

## 70 INTRODUCTION

71 The COVID-19 pandemic has taken an unprecedented toll on lives, wellbeing,  
72 healthcare systems, and global economies. As of 1 September 2020, there have been  
73 more than 25.5 million confirmed cases globally with more than 850,000 confirmed  
74 deaths<sup>1</sup>. However, these numbers and the current mapping of disease spread present an  
75 incomplete picture of the outbreak largely due to the lack of adequate testing, particularly  
76 as undetected infected cases are the main source of disease spread<sup>2-7</sup>. It is estimated  
77 that the reported detection rate of actual COVID-19 cases is only 1-2%<sup>5</sup>. As of September  
78 2020, the United States and Brazil remain the top two countries with the highest number  
79 of COVID-19 cases and deaths worldwide. As countries begin to re-open their economies,  
80 a method for accessible and frequent surveillance of COVID-19, with the necessary rapid  
81 quarantine measures, is crucial to prevent the multiple resurgences of the disease.

82 The current standard of care rightfully places a strong focus on the diagnostic limit  
83 of detection, yet frequently at the expense of both cost and turnaround time. This situation  
84 has contributed to limited population testing largely due to a dearth of diagnostic  
85 resources. Quantitative real-time polymerase chain reaction (qRT-PCR) is the gold-  
86 standard method for clinical diagnosis, with high sensitivity and specificity, but these tests  
87 are accompanied by the need for trained personnel, expensive reagents and  
88 instrumentation, and a significant amount of time to execute. Facilities offering qRT-PCR  
89 sometimes require a week or longer to complete and return the results to the patient.  
90 During this waiting period the undiagnosed individual may spread the infection and/or  
91 receive delayed medical treatment. Moreover, due to the cost and relative inaccessibility  
92 of qRT-PCR in both resource-limited and abundant settings, large-scale screening using

93 qRT-PCR at frequent intervals remains impractical as a way to identify infected but  
94 asymptomatic or mildly symptomatic infections. Numerous studies have reported  
95 asymptomatic COVID-19 cases as well as a variation in viral load within and between  
96 individuals at different time points, suggesting the need for more frequent testing for  
97 informative surveillance.

98 Technologies alternate to qRT-PCR, such as rapid viral antigen detection,  
99 clustered regularly interspaced short palindromic repeats (CRISPR), and loop-mediated  
100 isothermal amplification (LAMP) of SARS-CoV-2 provide potential large-scale screening  
101 applications, yet their implementation is stymied by requirements for qRT-PCR-like  
102 accuracy before they can reach the market<sup>8</sup>. In countries such as India, where the qRT-  
103 PCR resources would not be sufficient to cover monitoring of the population, the use of  
104 rapid antigen tests is well underway<sup>9,10</sup>. In early May 2020, the United States Food and  
105 Drug Administration (FDA) authorized the first antigen test for the laboratory detection of  
106 COVID-19, citing a need for testing beyond molecular and serological methods. Antigen  
107 testing detects the viral proteins rather than nucleic acids or human antibodies, allowing  
108 for detection of an active infection with relative ease of sample collection and assay.  
109 These rapid assays – like other commercially-available rapid antigen tests - can be mass-  
110 produced at low prices and be administered by the average person without a laboratory  
111 or instrumentation. These tests also take as little as 15 minutes to determine the result,  
112 enabling real-time surveillance and/or diagnosis. Although antigen tests usually perform  
113 with high specificities (true negative rate), their sensitivity (true positive rate) is often lower  
114 when compared to molecular assays. While qRT-PCR can reach a limit of detection as

115 low as  $10^2$  genome copies per mL<sup>11</sup>, rapid antigen testing detects viral protein that is  
116 assumed to correlate with approximately  $10^5$  genome copies per mL.

117 We hypothesize that frequent antigen-based rapid testing even with lower  
118 sensitivities compared to qRT-PCR - along with appropriate quarantine measures - can  
119 be more effective at decreasing COVID-19 spread than less frequent molecular testing of  
120 symptomatic individuals. Keeping in mind the realities of daily testing in resource-limited  
121 regions, we also hypothesize that testing frequency can be adjusted according to the  
122 prevalence of the disease; that is, an uptick in reported cases should be accompanied by  
123 more frequent testing. During the viral incubation period, peak infectivity correlates with  
124 a high viral load that can be detected by either qRT-PCR or rapid antigen testing<sup>12-15</sup>.  
125 Rapid tests thus optimize diagnosis for the most infectious individuals. Studies also point  
126 to the relatively small window of time during an individual's incubation period in which the  
127 qRT-PCR assay is more sensitive than rapid tests<sup>12</sup>.

128 In this study we report the development and clinical validation of a direct antigen  
129 rapid test for detection of SARS-CoV-2 spike glycoprotein using 121 retrospectively  
130 collected nasopharyngeal swab specimens. Using the clinical performance data, we  
131 develop a modeling system to evaluate the impact of frequent rapid testing on COVID-19  
132 spread and outcomes using a variation of a SIR model, which has been previously used  
133 to model COVID-19 transmission<sup>16-22</sup>. We build on this model to incorporate quarantine  
134 states and testing protocols to examine the effects of different testing regimes. This model  
135 distinguishes between undetected and detected infections and separates severe cases,  
136 specifically, those requiring hospitalization, from those less so, which is important for  
137 disease response systems such as intensive care unit triaging. We simulate COVID-19

138 spread with rapid testing and model disease outcomes in three regions in the United  
139 States and São José do Rio Preto, Brazil - the site of the clinical validation study - using  
140 publicly available data. To date, COVID-19 modeling describes the course of disease  
141 spread in response to social distancing and quarantine measures, and a previous  
142 simulation study has shown that frequent testing with accuracies less than qRT-PCR,  
143 coupled with quarantine process and social distancing, are predicted to significantly  
144 decrease infections<sup>12,16,22-26</sup>. This is the first modeling system using publicly-available  
145 data to simulate how potential public health strategies based on testing performance,  
146 frequency, and geography impact the course of COVID-19 spread and outcomes. Our  
147 findings suggest that a rapid test, even with sensitivities lower than molecular tests, when  
148 strategically administered 2-3 times per week, will diminish COVID-19 spread,  
149 hospitalizations, and deaths at a fraction of the cost of nucleic acid testing via qRT-PCR.

150

## 151 **RESULTS**

### 152 **Direct Antigen Rapid Test Accuracy Correlates with Viral Load Levels**

153 Rapid antigen tests have recently been considered a viable source for first-line  
154 screening, although concerns about the accuracy of these tests persist. We developed a  
155 direct antigen rapid test in a lateral flow dipstick format for the detection of the spike  
156 glycoprotein from SARS-CoV-2 in nasopharyngeal swab specimens. Of the total number  
157 of nasopharyngeal swab specimens evaluated by qRT-PCR for amplification of SARS-  
158 CoV-2 RNA-dependent RNA polymerase (RdRp), nucleocapsid (N), and envelope (E)  
159 genes, 72 tested positive and 49 tested negative (Table 1).

160 The overall sensitivity and specificity of the rapid antigen test was 84.7% and  
 161 85.7%, respectively (Table 1). Our data demonstrate that the sensitivity of our test is  
 162 positively correlated to the viral load level (Fig. 1, Table 2). The rapid test result was  
 163 compared to the qRT-PCR cycle threshold (Ct) value measured across RdRp, N, and E  
 164 genes, and calculated as sensitivity and specificity.

165  
 166

**Table 1.** Clinical validation summary for the SARS-CoV-2 direct antigen rapid test (DART) evaluated using 121 retrospectively collected patient nasopharyngeal swab specimens.

167

All Data Summary							
		qRT-PCR (gene average)			95% Confidence Interval		
		+	-	Total	Sensitivity	84.7%	80.6% - 88.9%
DART	+	61	7	68	Specificity	85.7%	80.8% - 90.6%
	-	11	42	53	Positive Predictive Value	89.7%	86.2% - 93.2%
Total		72	49	121	Negative Predictive Value	79.2%	73.6% - 84.9%
					Prevalence	59.5%	53.9% - 65.1%
					Overall Agreement	85.1%	82.0% - 88.3%

168

169

170

171

172

173

174

175

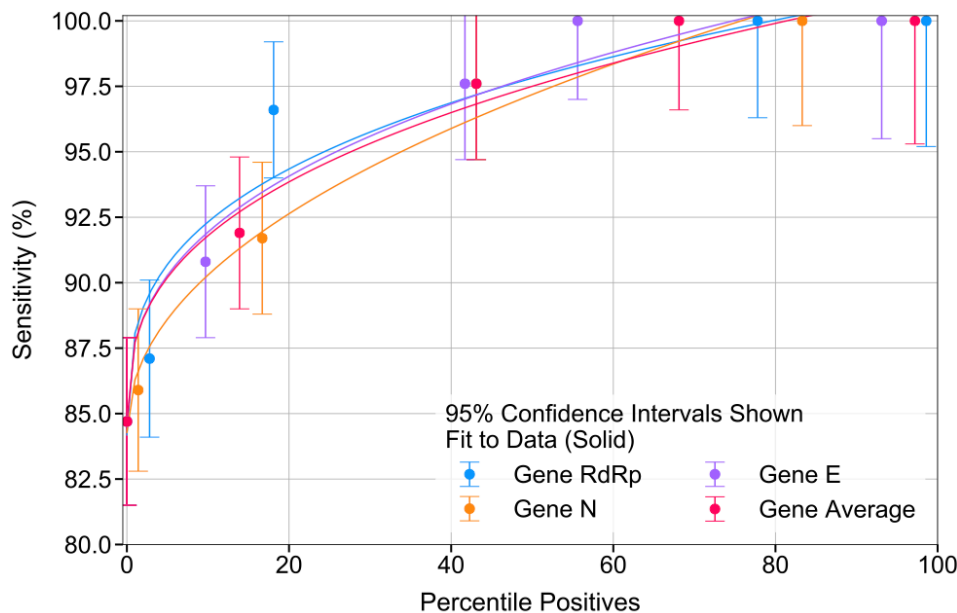


**Table 2.** Data summary of direct antigen rapid test (DART) performance in comparison to qRT-PCR results; for each gene being detected and amplified by qRT-PCR (E: envelope, N: nucleocapsid, RdRp: RNA-dependent RNA polymerase, and average), DART performance is organized by qRT-PCR Cycle threshold value increments.

176

	Cycle threshold (Ct) value	Total Cases	DART Positives	DART Negatives	Percentile Positives in Total Population	Sensitivity	95% Confidence Interval (semi-interval)	Specificity	95% Confidence Interval (semi-interval)	Positive Predictive Value (PPV)	Negative Predictive Value (NPV)	Prevalence	Overall Agreement	
SARS-CoV-2 qRT-PCR	RdRp gene	< 10	1	49	98.6%	100.0%	30.0%	85.7%	4.9%	12.5%	100.0%	2.0%	86.0%	
		< 15	16	49	77.8%	100.0%	3.9%	85.7%	4.9%	69.6%	100.0%	24.6%	89.2%	
		< 20	41	49	43.1%	97.6%	2.8%	85.7%	4.9%	85.1%	97.7%	45.6%	91.1%	
		< 25	59	49	18.1%	96.6%	2.5%	85.7%	4.9%	89.1%	89.1%	54.6%	91.7%	
		< 30	121	72	2.8%	84.7%	4.1%	85.7%	4.9%	89.7%	79.2%	59.5%	85.1%	
		< 35	121	72	0.0%	84.7%	4.1%	85.7%	4.9%	89.7%	79.2%	59.5%	85.1%	
	N gene	< 10	49	0	49	100.0%	-	-	85.7%	4.9%	0.0%	100.0%	0.0%	85.7%
		< 15	61	12	49	83.3%	100.0%	5.1%	85.7%	4.9%	63.2%	100.0%	19.7%	88.5%
		< 20	90	41	49	43.1%	97.6%	2.8%	85.7%	4.9%	85.1%	97.7%	45.6%	91.1%
		< 25	109	60	49	16.7%	91.7%	3.5%	85.7%	4.9%	88.7%	89.4%	55.0%	89.0%
		< 30	120	71	49	1.4%	85.9%	4.0%	85.7%	4.9%	89.7%	80.8%	59.2%	85.8%
		< 35	121	72	49	0.0%	84.7%	4.1%	85.7%	4.9%	89.7%	79.2%	59.5%	85.1%
E gene	< 10	54	5	49	93.1%	100.0%	10.8%	85.7%	4.9%	41.7%	100.0%	9.3%	87.0%	
	< 15	81	32	49	55.6%	100.0%	2.0%	85.7%	4.9%	82.1%	100.0%	39.5%	91.4%	
	< 20	91	42	49	41.7%	97.6%	2.7%	85.7%	4.9%	85.4%	97.7%	46.2%	91.2%	
	< 25	114	65	49	9.7%	90.8%	3.5%	85.7%	4.9%	89.4%	87.5%	57.0%	88.6%	
	< 30	121	72	49	0.0%	84.7%	4.1%	85.7%	4.9%	89.7%	79.2%	59.5%	85.1%	
	< 35	121	72	49	0.0%	84.7%	4.1%	85.7%	4.9%	89.7%	79.2%	59.5%	85.1%	
Gene Average	< 10	51	2	49	97.2%	100.0%	20.9%	85.7%	4.9%	22.2%	98.9%	3.9%	86.3%	
	< 15	72	23	49	68.1%	100.0%	2.8%	85.7%	4.9%	76.7%	98.9%	31.9%	90.3%	
	< 20	90	41	49	43.1%	97.6%	2.8%	85.7%	4.9%	85.1%	96.6%	45.6%	91.1%	
	< 25	111	62	49	13.9%	91.9%	3.4%	85.7%	4.9%	89.1%	89.4%	55.9%	89.2%	
	< 30	121	72	49	0.0%	84.7%	4.1%	85.7%	4.9%	89.7%	79.2%	59.5%	85.1%	
	< 35	121	72	49	0.0%	84.7%	4.1%	85.7%	4.9%	89.7%	79.2%	59.5%	85.1%	

177



178

**Figure 1.** Performance of direct antigen rapid test (DART) for the detection of SARS-CoV-2 in 121 retrospectively collected patient nasopharyngeal swab specimens. Percentile Positive ranks the samples in order of high Cycle threshold (Ct) value to low Ct value. DART sensitivity is determined by calculating true positive agreement to qRT-PCR; the plot uses an  $ax^b+c$  fit and 95% confidence intervals for the sensitivity. Shown are the percentile positive cases of the total positive population conditioned to qRT-PCR Ct for RdRp (RNA-dependent RNA polymerase), N (nucleocapsid), and E (envelope) genes, and the average of these genes.

179

180 Ct value cutoffs represent the number of qRT-PCR cycles at which generated  
181 fluorescence crosses a threshold during the linear amplification phase. The x-axis of  
182 Figure 1 describes the percentile positives in the total positive population. Percentile  
183 Positives ranks the samples in order of high qRT-PCR Ct value to low. In other words,  
184 the higher the percentile, the more “positive” because fewer qRT-PCR cycles are required  
185 for gene detection. Because the Ct value is a variable unit based upon qRT-PCR protocol  
186 and instrumentation, we evaluated sensitivity against the percentile of cases across Ct  
187 values.

188 As the percentile positive increases, the sensitivity between the rapid test and the  
189 gold-standard qRT-PCR increases, reaching 100% sensitivity at 68.1% percentile

190 positive for the gene average detection. Significantly, even at percentile positives  
191 between 0% and 68.1%, the sensitivity remains above 80%. Taken together, the clinical  
192 data shows that the rapid antigen test performs with increasing accuracy for individuals  
193 with a higher viral load, and are thus the most infectious<sup>13-15</sup>.

194

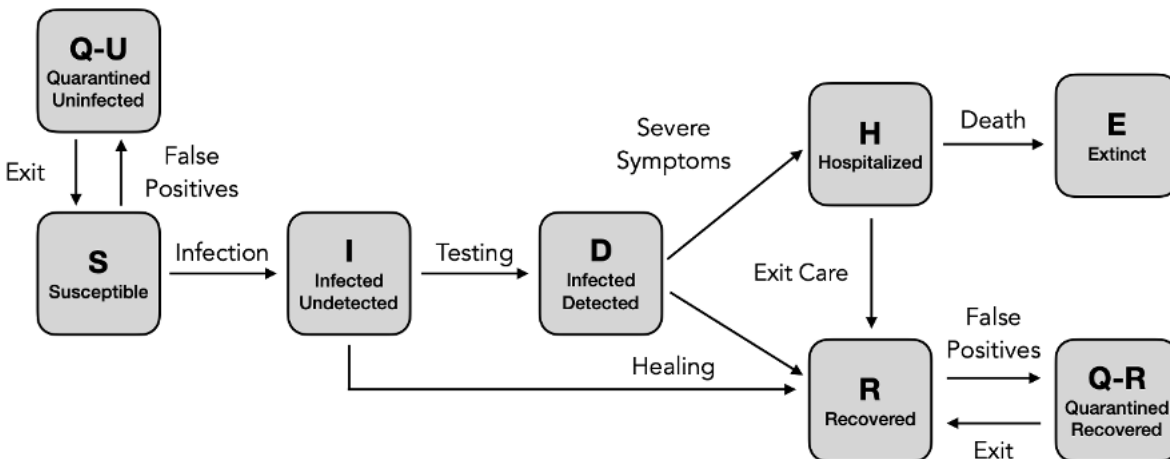
### 195 **An Enhanced Epidemiological SIDHRE-Q Model**

196 We propose an enhanced epidemiological modeling system, *SIDHRE-Q*, a variant  
197 of the classical SIR model in order to expand our clinical validation study and to  
198 understand the effects of using frequent rapid tests such as the rapid antigen test on  
199 COVID-19 outbreak dynamics. The changes we make to the basic model to encompass  
200 the unique characteristics of the COVID-19 pandemic are similar to those presented by  
201 Giordano et al.<sup>16</sup> (Fig. 2). The differential equations governing the evolution of the  
202 *SIDHRE-Q* model and descriptions of the parameter values are provided in the material  
203 and methods section (Equation 2, Table 5).

204

205

206



207

**Figure 2.** Graphical scheme displaying the relationships between the stages of quarantine and infection in *SIDHRE-Q* model: **Q-U**, quarantine uninfected; **S**, susceptible (uninfected); **I**, infected undetected (pre-testing and infected); **D**, infected detected (infection diagnosis through testing); **H**, hospitalized (infected with life threatening symptom progression); **R**, recovered (healed); **E**, extinct (dead); and **Q-R**, quarantine recovered (healed but in quarantine by false positive testing).

**Figure Supplement 1.** Graphical scheme displaying parameters between the stages of quarantine and infection in *SIDHRE-Q* model.

208

209

210 An individual that begins in **S** may either transition to a Quarantine Uninfected (**Q-**  
 211 **U**) state via a false positive result or to an Infected Undetected (**I**) state via interaction  
 212 with an infected individual. Should an individual in **S** move into **Q-U**, they are quarantined  
 213 for 14 days before returning to **S**, a time period chosen based on current knowledge of  
 214 the infectious period of the disease. One could also conceive of an effective strategy in  
 215 which individuals exit quarantine after producing a certain number of negative rapid tests  
 216 in the days following their initial positive result or confirm their negative result using qRT-  
 217 PCR.

218           Given that those diagnosed are predominantly quarantined, individuals in **I** interact  
219 more with the **S** population than do those in Infected Detected (**D**). Therefore, the  
220 infectious rate for **I** is assumed to be significantly larger than for **D**. Furthermore, a region's  
221 ability to control an outbreak is directly related to how quickly and effectively people in **I**  
222 test into **D**, reducing their infectiousness through quarantine. This study, in particular,  
223 highlights the critical role frequency of testing, along with strict quarantine, has in  
224 mitigating the spread of the disease and provides specific testing strategies based on  
225 rapid tests we predict to be highly effective.

226           In this model, we assume that individuals receive a positive diagnosis before  
227 developing severe symptoms and that those with symptoms severe enough to be  
228 potentially fatal will go to the hospital. If an individual develops symptoms, we assume  
229 they are tested daily until receiving a positive result; hence, before severe symptoms  
230 develop, they will be diagnosed with high probability. Those who do not develop  
231 symptoms are tested according to the frequency of tests administered to the general  
232 population. Therefore, there is no modeled connection between **I** and **H** or between **I** and  
233 **E**. Removing these assumptions would have negligible impact on the results as these  
234 flows are very small.

235           Should an individual test positive and transition to **D**, they may either develop  
236 serious symptoms requiring care or recover. Those who develop serious symptoms and  
237 transition to state **H** will then transition to either **R** or **E**. The recovered population is  
238 inevitably tested, as infected individuals may recover without being detected. Therefore,  
239 the Quarantined Recovered (**Q-R**) state is introduced with the same connections to **R** as  
240 the connections between **S** and **Q-U**. Though the reinfection rate of SARS-CoV-2 has

241 been a point of recent debate, it is assumed that the number of re-infected individuals is  
242 small<sup>27–31</sup>. Therefore, individuals cannot transition from **R** to **S**, hence the separately  
243 categorized quarantined populations.

244 We considered several variations and extensions of the *SIDHRE-Q* model. In  
245 simulations, we tested additional states, such as those in the *SIDARTHE* model, which  
246 include distinctions between symptomatic and asymptomatic cases for both detected and  
247 undetected populations<sup>16</sup>. Incorporating information about the correlations between viral  
248 load and infectivity and sensitivity were also considered. Altogether, our modeling system  
249 has been well tuned to predict the impact of high frequency rapid testing on COVID-19  
250 spread and outcomes.

251

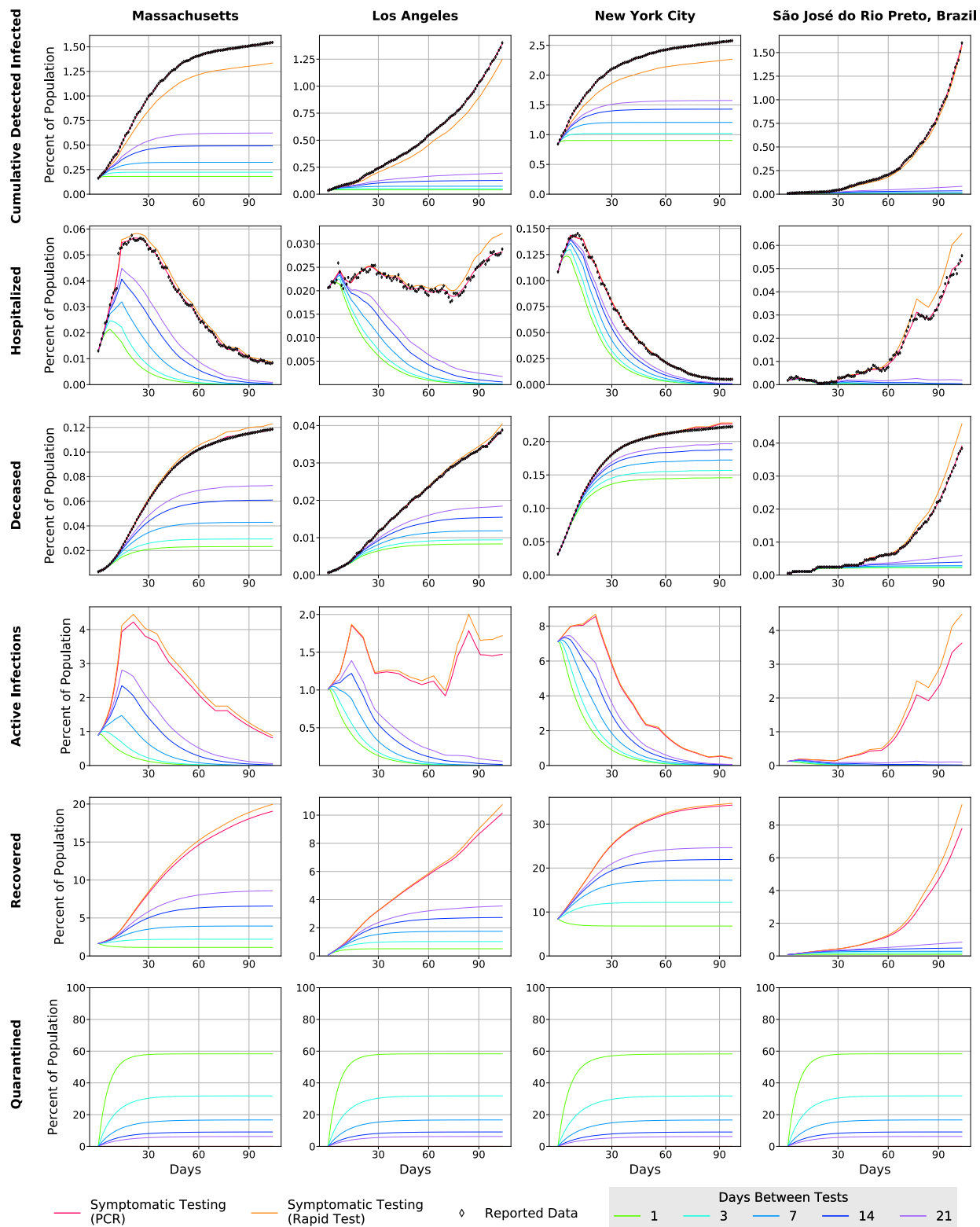
## 252 **Frequent Rapid Testing with Actionable Quarantining Dramatically Reduces** 253 **Disease Spread**

254 In order to demonstrate how strategies could affect the disease spread in different  
255 geographies and demographics, we used surveillance data obtained from regions of  
256 varying characteristics: the state of Massachusetts (MA), New York City (NYC), Los  
257 Angeles (LA), and São José do Rio Preto (SJRP), Brazil, the site of the rapid antigen test  
258 clinical validation study. These regions are also selected in our study due to the readily  
259 available surveillance data provided by the local governments. We fit the model to the  
260 data from each region starting 1 April 2020. At this time point the disease reportedly is  
261 most advanced in NYC and least advanced in SJRP, Brazil with estimated cumulative  
262 infection rates of 7.11% and 0.12%, respectively.

263           After calibrating the *SIDHRE-Q* model, the disease spread is observed with varying  
264 validated rapid antigen test performances and frequencies (Fig. 3). Sensitivity (the ratio  
265 of true positives to the total number of positives) and specificity (the ratio of true negatives  
266 to the total number of negatives) compared to gold-standard qRT-PCR were used as  
267 measures of test accuracy.

268           The rapid test frequency is varied while maintaining an accuracy of 80% sensitivity  
269 and 90% specificity, comparable to our clinical data collected in SJRP, Brazil. These  
270 testing scenarios are then compared to symptomatic testing, in which individuals receive  
271 a rapid test only when presenting symptoms, via either a rapid test or qRT-PCR. Since  
272 the primary testing regiment deployed in MA, LA, NYC and SJRP, Brazil is qRT-PCR-  
273 based and focused on symptomatic individuals, the symptomatic testing protocol via qRT-  
274 PCR is directly estimated from the data to be the rate  $\nu$  (Table 5).

275           The difference between the qRT-PCR and rapid test simulations (red and orange  
276 lines, respectively) is therefore only sensitivity of testing (Fig. 3). We assumed that test  
277 outcome probability is a function only of whether an individual is infected and independent  
278 of other factors; one can consider this a lower bound on effectiveness of a strategy, as  
279 sensitivity and infectivity are often positively correlated with antigen testing.



Sensitivity: 80.0% Specificity: 90.0%



**Figure 3.** COVID-19 Outcomes in 3 US Regions and Brazil as a result of Frequent Rapid Testing Protocol using the *SIDHRE-Q* Model. The Cumulative Detected Infected, Hospitalized, Deceased, Active Infections, Recovered, and Quarantined are modeled over 105 days (top to bottom) using reported data from 4 global regions: Massachusetts, Los Angeles, New York City, and São José do Rio Preto in Brazil (left to right). The COVID-19 population spread and outcomes are modeled under a Rapid Testing Protocol (sensitivity 80%, specificity 90%) with variable testing frequencies ranging from 1-21 days between tests. This protocol is compared to a symptom-based Rapid Testing protocol and a symptom-based qRT-PCR protocol.

**Figure Supplement 1.** COVID-19 Outcomes as a result of Frequent Rapid Testing Protocol with variable test performances using *SIDHRE-Q* Model.

**Figure Supplement 2.** Time series of the four fitted parameters  $\alpha$ ,  $\nu$ ,  $\mu$ , and  $\tau$ .

281

282

283 To better understand the effect of rapid testing frequency and performance on  
 284 healthcare capacity and mortality rates, we simulate the testing strategy with 30%-90%  
 285 sensitivity each with 80% or 90% specificity against the symptomatic testing strategy.  
 286 Table 3 describes the different test performances implemented in the model matched with  
 287 corresponding Figure 3 - Figure Supplement 1 plots.

**Table 3.** Test Performance with corresponding Figure 3 - Figure Supplement 1 designation.

288

Sensitivity (%)	Specificity (%)	Fig. 3 Supplemental Fig.
90	90	1A
70	90	1B
50	90	1C
30	90	1D
90	80	1E
70	80	1F
50	80	1G
30	80	1H

289

290

291 As per our hypothesis, frequency and symptom-based testing dramatically  
292 reduced infections, simultaneous hospitalizations, and total deaths when compared to the  
293 purely symptom-based testing regiments, and infections, hospitalization, and death were  
294 reduced as frequency increased. Although testing every day was clearly most effective,  
295 even testing every fourteen days with an imperfect test gave an improvement over  
296 symptomatic testing with qRT-PCR. While the strategy works best when implemented at  
297 the very beginning of an outbreak, as demonstrated by the results in SJRP, Brazil, it also  
298 works to curb an outbreak that is already large, as demonstrated by the results in NYC.  
299 The difference between frequencies is more noticeable when the testing strategy is  
300 applied to the outbreak in NYC, leading us to hypothesize that smaller outbreaks require  
301 a lower testing frequency than larger ones; note the difference between the dependence  
302 on frequency to curb a small initial outbreak in SJRP, Brazil versus a large one in NYC  
303 (Fig. 4, Figure 4 - Figure Supplement 1).

304 For test performance of 80% sensitivity and 90% specificity, the percent of the  
305 population that has been infected in total from the beginning of the outbreak to mid-July  
306 drops from 18% (MA), 11% (LA), 26% (NYC), and 11% (SJRP, Brazil) to 3%, 2%, 12%,  
307 and 0.26%, respectively, using a weekly rapid testing and quarantine strategy (with  
308 regards to predictions of overall infection rates, other studies based on seroprevalence  
309 and epidemiological predictions have reached similar conclusions<sup>32,33</sup>). If testing is  
310 increased to once every three days, these numbers drop further to 1.6% (MA), 1.4% (LA),  
311 9.4% (NYC), and 0.19% (SJRP, Brazil) (Table 4).

312

**Table 4.** Summary of results of COVID-19 outcomes in 3 US Regions and Brazil as a result of Frequent Rapid Testing Protocol using SIDHRE-Q Model.

313

	Massachusetts		Los Angeles		New York City		São José do Rio Preto, Brazil	
	qRT-PCR	1 per 3 days	qRT-PCR	1 per 3 days	qRT-PCR	1 per 3 days	qRT-PCR	1 per 3 days
<b>Total Infected</b>	18.40%	1.60%	11.70%	1.42%	26.40%	9.45%	11.70%	0.186%
<b>Max Hospitalized</b>	0.056%	0.025%	0.028%	0.022%	0.144%	0.130%	0.054%	0.003%
<b>Total Deaths</b>	0.119%	0.029%	0.039%	0.009%	0.226%	0.157%	0.040%	0.003%

314

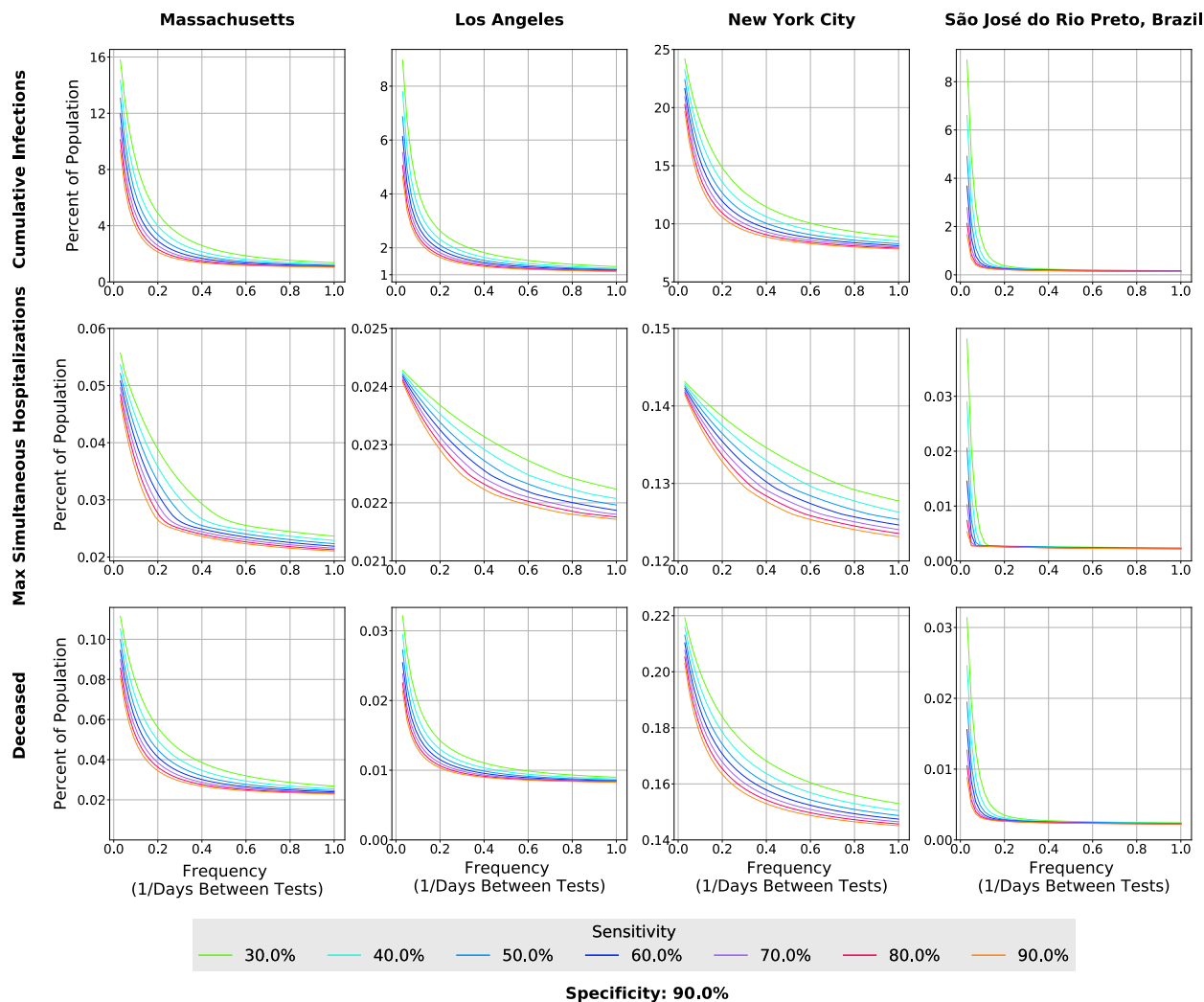
315

316 To further examine the relationship between frequency and sensitivity, we modeled  
 317 the maximum number of individuals in a given state over the 105-day time period for four  
 318 geographic regions (Fig. 4). In all four geographic regions, as frequency of testing  
 319 increases, the total infections, maximum simultaneous hospitalizations, and total deaths  
 320 converge to small percentages regardless of the sensitivity at high frequencies. It is clear  
 321 that the difference in frequency required to achieve the same result using tests of differing  
 322 sensitivities is very small (Fig. 4) For example, we predict that for the outbreak in LA, a  
 323 testing strategy started on 1 April of every 10 days using a test of sensitivity 90% would  
 324 have resulted in 2.5% of the population having been infected, while using a test of  
 325 sensitivity 30% would require a strategy of every 5 days to achieve the same number.  
 326 Thus, we conclude that frequency is more important than sensitivity in curbing the spread,  
 327 and a large range of sensitivities prove effective when testing sufficiently often. How  
 328 frequently, exactly, depends on the specific outbreak and what stage it is in, which leads  
 329 us to the location-based deployment strategy discussed in a later section. Frequency of

330 testing can be significantly reduced to effectively contain the disease once the initial  
331 outbreak has been controlled; it is clear that this takes only a matter of weeks (Fig. 3).

332 On the other hand, according to the specificity of the rapid test and the quarantine  
333 duration, larger testing frequency result in a larger percent of the population quarantined  
334 (Fig. 3). Assuming a 90% rapid test specificity and 14-day quarantine duration, for the 1-  
335 , 3- and 7-day frequencies almost 60%, 38% and 20% of the population, respectively,  
336 would be quarantined. This figure may be reduced with additional rules for exiting  
337 quarantine early, such as after complementary testing. An example of such a strategy is  
338 that individuals who test positive are required to either quarantine for two weeks or  
339 produce two consecutive negative rapid tests in the two days following their positive  
340 result. Assuming 80% sensitivity and 90% specificity, those individuals will reenter the  
341 public while still infected with probability 0.04. If uninfected, that individual will exit  
342 quarantine after two days with probability 0.81. However, a compromise between the  
343 reduction of infections and the proportion of the population in quarantine would be part of  
344 the planning for the appropriate testing protocol in each community or region.

345 Additionally, while high frequency may be necessary to contain a large outbreak  
346 initially, relatively infrequent testing, such as every one or two weeks, is sufficient to keep  
347 controlled outbreaks small, while reducing the number of quarantined individuals to less  
348 than 10% of the population using a two-week mandatory quarantine.



349

**Figure 4.** Effect of Rapid Testing Protocol under variable testing sensitivities and increasing frequency under the *SIDHRE-Q* Model. The Cumulative Infections, Maximum Simultaneously Hospitalized, and Deceased populations are modeled for Massachusetts, Los Angeles, New York City, and São José do Rio Preto in Brazil. The effect of increasing frequency of testing is modeled for various testing sensitivities (30%-90%) with a 90% specificity.

**Figure 4 - Figure Supplement 1.** Effect of Rapid Testing Protocol under variable testing sensitivities and increasing frequency under the *SIDHRE-Q* Model (80% specificity).

350

351

352

353

354

## 355 **A County-Based Testing Strategy Offers a Cost-effective Approach to Large-scale** 356 **COVID-19 Surveillance**

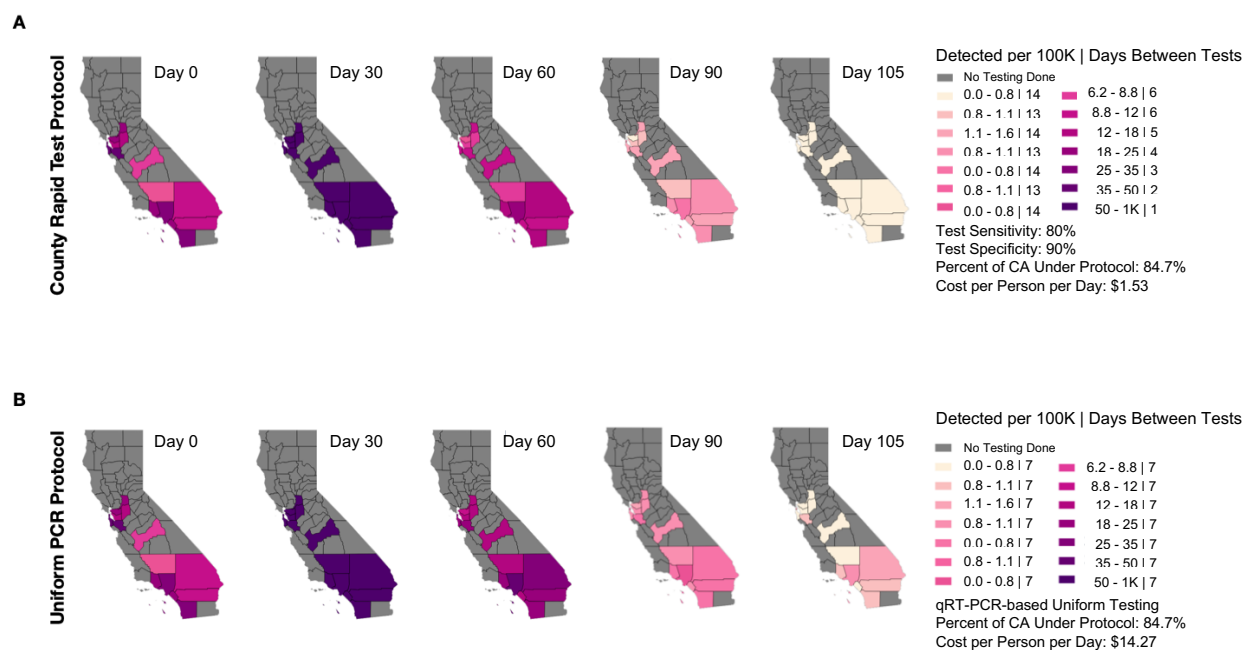
357 To examine the effects of resource-strategic testing schemes, we modeled the  
358 COVID-19 prevalence by varying testing frequency across counties of California. For this  
359 analysis, only California was analyzed because of the accessibility of the county level  
360 data. In this scheme, the percent of active infected detected individuals in a county  
361 determines the frequency of testing. We define thresholds for the number of active  
362 detected infections that, when hit, initiate testing protocols of different frequencies  
363 depending on the threshold hit. We first tested evenly spaced thresholds for the number  
364 of detected active infections up to 1% of the population, but later adopted thresholds that  
365 were determined according to Equation 1. In Equation 1,  $D$  = population of state  $D$  at the  
366 time of testing.  $T$  = number of active infections which, if reached, initiates everyday  
367 testing. The days between tests are rounded to the closest integer value.

$$\text{Days between tests} = \max(1, 2 \log_2(T/D) + 1)$$

368  
369 (1)

370 The days between tests are chosen such that the detected active infections should  
371 remain near to or below  $T$ . If the initial detected active infections are greater than  $T$ , then  
372 the testing frequency of 1 will cause infections to rapidly drop. Both the threshold at which  
373 everyday testing begins and the coefficient of  $\log_2 T/D$  can be modified to produce a  
374 strategy that is more or less frequent in testing or resource effective; a range of days  
375 between tests from 14 days to 1 day are used (Fig. 5). A scan over different choices of  $T$   
376 is shown in the supplements to Figure 5; the threshold we choose in Figure 5 is 0.05%  
377 because it is successful in curbing the outbreak within the time period we consider. While

378 these choices work for the epidemic in California at the point we start our simulations, 10  
 379 April, they do not necessarily reflect the most resource effective choices everywhere. Our  
 380 analysis could be redone to select the best strategy in other states or in the country as a  
 381 whole.



382

**Figure 5.** Effect of County Based Rapid Test Protocol (A) and Uniform qRT-PCR Protocol (B) on active infected detected population over time in California (CA). The legend denotes the thresholds at which testing frequency is determined, the testing frequencies, the percent of CA population under the strategy, and the cost per person per day.

**Figure Supplement 1.** Effect of County Based Rapid Testing strategy on COVID-19 outcomes in California.

**Figure Supplement 2.** Time series of the three fitted pieces of data Cumulative Cases, Daily Hospitalized, and Cumulative Deaths for each CA county receiving testing.

383

384 Using a rapid test with a sensitivity of 80% and specificity of 90%, the county-based  
 385 testing with threshold 0.05% reduces the active infections from 0.94% to 0.0005%, while  
 386 the uniform strategy with tests administered every 7 days results in double the number of  
 387 active infections (Fig. 5). As the threshold is reduced, the total cost increases while the

388 cumulative infections, maximum percentage hospitalized, and cumulative deaths all  
389 decrease (Figure 5 - Figure Supplement 1).

390 Strategy B in Figure 5 consists of qRT-PCR testing uniformly applied to the  
391 highlighted population with a frequency of once weekly. The average cost per person per  
392 day is just under \$15. Despite this frequency and the accuracy of qRT-PCR, the strategy  
393 does not succeed in curbing the spread as fast as strategy A, which uses a testing  
394 sensitivity and specificity of 80% and 90%, respectively, and testing frequency that vary  
395 between counties depending on the proportion of their population that is currently  
396 infected. The total cost for strategy A is estimated at a fraction of the other at \$1.53 per  
397 person per day.

398  
399

## 400 **DISCUSSION**

401 In this study we examine the potential effects of a novel testing strategy to limit the  
402 spread of SARS-CoV-2 utilizing rapid antigen test screening approaches. Our clinical data  
403 and *SIDHRE-Q* modeling system demonstrate that 1) frequent rapid testing even at a  
404 range of accuracies is effective at reducing COVID-19 spread, 2) rapid antigen tests are  
405 a viable source for this strategy and diagnose the most infectious individuals, and 3)  
406 strategic geographic-based testing can optimize disease control with the amount of  
407 available resources. The information from a diagnostic test itself is of tremendous value,  
408 as it can prompt the necessary quarantine measures to prevent spread, guide proper care  
409 and triage, and provide crucial disease-tracking information. Diagnostic testing in the  
410 United States and abroad, however, has been a significant public health hurdle. The  
411 public has witnessed and experienced symptomatic individuals being denied testing due



412 to shortages, and few testing structures for asymptomatic or mildly symptomatic  
413 individuals - the main source of disease spread. Though several factors contributed to the  
414 stymied early response measures, such as lockdown and quarantine protocols and  
415 adherence, severe testing bottlenecks were a significant culprit<sup>34-36</sup>. Early control  
416 measures have been shown to decrease lives lost by several orders of magnitude<sup>37</sup>.  
417 These challenges, though exacerbated during the early months of the pandemic, remain  
418 at the forefront of the public health crises.

419         Diagnosis of SARS-CoV-2 infection by qRT-PCR is the current standard of care,  
420 yet remains expensive and requires a laboratory and experienced personnel for sample  
421 preparations and experimentation. Significantly, the turnaround time for results can be up  
422 to 10 days<sup>38</sup>. On an individual scale, this leaves the public in limbo, preventing people  
423 from either leaving quarantine if they are negative, or delaying critical care and infecting  
424 others if they are positive. On a societal level, this current testing scheme yields  
425 incomplete surveillance data on which response efforts such as societal reopening and  
426 hospital management depend. Though qRT-PCR is considered the gold-standard  
427 diagnostic method because of its high sensitivity and specificity, the logistical hurdles  
428 render it unrealistic for large-scale screening.

429         As qRT-PCR remains impractical for this strategy, and rapid tests are facing  
430 regulatory challenges because they do not perform with qRT-PCR-like accuracy, rapid  
431 test screening is either nonexistent in several countries or symptom-based. Even under  
432 best-case assumptions, findings have shown that symptom and risk-based screening  
433 strategies miss more than half of the infected individuals<sup>39</sup>. Some have argued that the  
434 need for widespread testing is overstated due to the variability in test sensitivity and

435 specificity<sup>40</sup>. Our findings show, however, that test performance, though valuable, is  
436 secondary to widespread test frequency, which is enabled by accessibility and turnaround  
437 time.

438 Giordano et al. has modeled the evolution of SARS-CoV-2 spread, introducing a  
439 diagnosed state to elucidate the importance of population-wide testing<sup>16</sup>. Mina et al. has  
440 examined how various test sensitivities and frequencies affect the reproductive number<sup>12</sup>.  
441 We build upon these findings to show how in affected United States and Brazil regions,  
442 population-wide frequent and rapid testing schemes, with sensitivities ranging from 30%-  
443 90%, can be more effective in curbing the pandemic than a PCR-based scheme.  
444 Integrating real-world surveillance and clinical data into our modeling system has allowed  
445 us to incorporate regional differences - such as variances in healthcare access, state  
446 health policy and adherence, state GDP, and environmental factors - under the same  
447 model. Significantly, our findings hold true across Massachusetts, New York City, Los  
448 Angeles, and São José do Rio Preto, Brazil. We also present the economic  
449 considerations of these testing regimes, showing that widespread rapid testing is more  
450 cost efficient than less frequent qRT-PCR testing. In line with these economic  
451 considerations, our model demonstrates the effectiveness of a geographic-based  
452 frequent testing regime, in which high disease prevalence areas receive more frequent  
453 testing than low disease prevalence areas.

454 Since COVID-19 is known to affect certain demographics differently, modeling  
455 would benefit from incorporating demographic information correlated with disease  
456 progression and spread to define sub-models and sets of parameters accordingly. Age,  
457 pre-existing conditions, job types, and density of population are examples of possible

458 categories, each of which influence the risk of contracting and/or dying from COVID-19.  
459 Further studies may benefit from incorporating these ideas should more information  
460 become available.

461 Our findings also point to low-cost tools for implementation of this testing strategy,  
462 such as a rapid antigen-based test for the detection of SARS-CoV-2 proteins. We show  
463 that the rapid antigen test performs with a range of accuracies under which disease  
464 spread can be dramatically mitigated under our model. Notably, the sensitivity is  
465 correlated to the individual's viral load, effectively diagnosing those who are most  
466 infectious with the highest accuracy. Our findings are significant because these rapid  
467 antigen tests are cheaper than qRT-PCR, can be mass produced to millions per day,  
468 present results within 15 minutes, and can be administered by a nonexpert without a lab  
469 or special equipment.

470 There are several policy implications for these findings. First, our model supports  
471 that systems of high frequency rapid testing should be implemented as a first-line  
472 screening method. This can be first enabled by a more holistic regulatory evaluation of  
473 rapid diagnostics, such that policy emphasizes accessibility and turnaround time even  
474 under a range of accuracies. One can imagine a less accurate, though rapid method of  
475 first-line screening in schools, public transportation, and airports, or even at home, and a  
476 qRT-PCR-based method for second-line screening (testing those who present severe  
477 symptoms or have been in contact with infected individuals, testing in a clinical setting,  
478 etc). Second, our cost analysis and rapid antigen test data present a viable and potentially  
479 more cost-effective method for screening. Third, our county-based testing scheme  
480 presents a possible method for wide-scale screening while optimizing resources. Future

481 studies should investigate how this selective testing strategy can be applied to different  
482 location scales to further inform health policy. Moreover, though our models analyze  
483 regions in the United States and Brazil, similar testing strategies can be considered  
484 globally in both resource limited and abundant settings due to the higher accessibility of  
485 rapid tests compared to qRT-PCR.

486 We emphasize that integral to the effectiveness of diagnostic schemes is 1) the  
487 proper adherence to quarantine measures and 2) the combined use of a variety of  
488 diagnostic methods including nucleic acid, antigen, and antibody tests. According to these  
489 models, rapid antigen tests are an ideal tool for first-line screening. Clinical molecular  
490 tests such as qRT-PCR are vital to the diagnostic landscape, particularly to re-test  
491 suspected cases that were negative on the rapid test. Because rapid tests present a  
492 higher rate of false negatives, methods such as qRT-PCR remain integral to second-line  
493 screening. Antibody tests provide important information for immunity and vaccination  
494 purposes as well as epidemiological surveillance. This model also assumes that  
495 individuals will quarantine themselves before being tested and for 14 days following a  
496 positive diagnostic result.

497 Our simulations combined with real-world data demonstrate a robust modeling  
498 system and elucidates the significance of this novel testing strategy. However, there are  
499 important limitations to be considered. Differences in disease reporting between the  
500 geographical regions and the incomplete nature of COVID-19 surveillance data, often due  
501 to the lack of testing, are not considered in the model. It is imperative that the testing  
502 results, hospitalization and death statistics, and changes in protocol are reported in real-  
503 time to scientists and policy makers so that models can be accurately tuned as the

504 pandemic develops. The model also does not take into account infrastructural limitations  
505 such as hospital capacity. Though the rapid antigen test offers several advantages such  
506 as affordability, fast turnaround time, and ease of mass production, we are also assuming  
507 that there are systems in place to implement frequent and safe low-cost screening across  
508 different communities and settings.

509 Our model underscores the need for a point-of-care or at-home test for frequent  
510 screening, particularly as lockdown restrictions ease. Regulatory agencies such as the  
511 FDA could work towards regulating rapid tests to alternative standards other than  
512 comparison to high sensitivity molecular diagnostics, as our model shows that frequency  
513 and scale of testing may overcome lower sensitivities. Rather, we could refocus policy to  
514 implement first-line screening that optimizes accuracy with efficiency and equitability.

515

## 516 **MATERIAL AND METHODS**

### 517 **Development of Direct Antigen Rapid Test for the Detection of SARS-CoV-2**

518 We developed a direct antigen rapid test for the detection of the spike glycoprotein  
519 from SARS-CoV-2 in nasopharyngeal swab specimens as previously described<sup>41</sup>. Briefly,  
520 the rapid antigen test is an immunochromatographic format with a visual readout using  
521 anti-spike mouse monoclonal antibodies (E25Bio, Inc., Cambridge, MA, USA) that are  
522 either coupled to 40 nm gold nanoparticles (Abcam, Cambridge, UK) or adsorbed to  
523 nitrocellulose membranes (Sartorius, Goettingen, Germany). Each rapid antigen test has  
524 a control area adjacent to the paper absorbent pad; the control is an anti-mouse Fc  
525 domain antibody (Leinco Technologies, Fenton, MO, USA) that will capture any of the  
526 antibody-conjugated gold nanoparticles to generate a control visual signal. A visual signal

527 at the test area reflects SARS-CoV-2 spike glycoprotein that is “sandwiched” between an  
528 anti-spike glycoprotein antibody adsorbed to the nitrocellulose membrane and a second  
529 anti-spike glycoprotein antibody covalently coupled to visible gold nanoparticles.

530

### 531 **Validation of Direct Antigen Rapid Test for the Detection of SARS-CoV-2**

532 In a retrospective study of nasopharyngeal swab specimens from human patients,  
533 we compared the accuracy of the rapid antigen test to the viral load of individuals.  
534 Nasopharyngeal swab specimens (n = 121) were tested in Brazil following approved  
535 human subjects use protocols. The age of study participants ranged from 1 to 95 years  
536 with an overall median of 37 years (interquartile range, 27–51 years), and 62% were  
537 female. The demographic summary of the patients are included in Supplementary Table  
538 1. The nasopharyngeal swab specimens were banked refrigerated or frozen samples  
539 from suspected patients submitted to the lab for routine COVID diagnosis. Prior to using  
540 the rapid test, the nasopharyngeal swab samples were validated by qRT-PCR using  
541 GeneFinder™ COVID-19 Plus RealAmp Kit (OSANGHealthcare, Anyang-si, Gyeonggi-do,  
542 Republic of Korea I). The primary study under which the samples and data were collected  
543 received ethical clearance from the Faculdade de Medicina de São José do Rio Preto  
544 (FAMERP), protocol number 31588920.0.0000.5415. All excess samples and  
545 corresponding data were banked and de-identified prior to the analyses.

546 A nasopharyngeal swab specimen (1 mL) was concentrated using a Vivaspin 500  
547 centrifugal concentrator (Sartorius, Goettingen, Germany) at 12,000 x g for 10 minutes.  
548 The concentrated nasopharyngeal swab specimen retentate was transferred to a  
549 collection tube and the rapid antigen test was inserted into the tube with the retentate and

550 allowed to react for 15 minutes. After processing of the rapid antigen test, the visual  
551 positive or negative signal was documented.

552

### 553 **Data for Modeling**

554 As of August 2020, the United States and Brazil have the highest number of  
555 confirmed COVID-19 cases and deaths worldwide, with both countries reporting their first  
556 case on 26 February 2020<sup>1</sup>. Although several affected US regions could have been  
557 modeled, we look at data from Massachusetts, New York, and Los Angeles: these regions  
558 each contained “hotspots”, or areas of surging COVID-19 cases, at different points in time  
559 during the pandemic and have publicly available government-provided surveillance data.  
560 Our model is fit using data over 105 days beginning on April 1 for Figures 3 and 4 and  
561 105 days beginning on April 10 for Figure 5 (see “Modeling Parameters” in Methods). In  
562 order to understand the various testing proposals on a global scale, we performed our  
563 clinical study in and expanded the modeling study to Brazil. The specific data we use to  
564 fit our model are cumulative confirmed cases, total deaths, and number of daily  
565 hospitalizations due to COVID-19. This surveillance data was retrieved from government-  
566 provided online databases<sup>42–48</sup>.

567

### 568 **Modeling Parameters**

569 Equation 2 below provides the exact differential equations governing the model.

$$\begin{aligned}
 d\mathbf{S} &= -\mathbf{S}(\alpha\mathbf{I} + \eta\mathbf{D} + \gamma) && + \psi\mathbf{Q}_U \\
 d\mathbf{I} &= -\mathbf{I}(\varepsilon + \lambda + \nu) && + \mathbf{S}(\alpha\mathbf{I} + \eta\mathbf{D}) \\
 d\mathbf{D} &= -\mathbf{D}\left(\frac{\mathbf{D} + \mathbf{I}}{\mathbf{D}}\mu + \rho\right) && + \mathbf{I}(\nu + \varepsilon) \\
 d\mathbf{H} &= -\mathbf{H}(\sigma + \tau) && + \mu(\mathbf{D} + \mathbf{I}) \\
 d\mathbf{E} &= && + \tau\mathbf{H} \\
 d\mathbf{R} &= -\gamma\mathbf{R} && + \rho\mathbf{D} + \lambda\mathbf{I} + \sigma\mathbf{H} + \psi\mathbf{Q}_R \\
 d\mathbf{Q}_U &= -\psi\mathbf{Q}_U && + \gamma\mathbf{S} \\
 d\mathbf{Q}_R &= -\psi\mathbf{Q}_R && + \gamma\mathbf{R}
 \end{aligned}
 \tag{2}$$

570

571 In order to determine the values of the parameters defining the flows between states, we  
 572 use a least squares regression performed at seven day intervals in the datasets to which  
 573 we fit. This allows the model to take into account the time dependent nature of the  
 574 parameters, which rely on factors such as social distancing regulations and changes in  
 575 testing capacity. We also fit window sizes between 1 and 21 days and find that while the  
 576 fit degrades with larger window size, the overall shape of the fits do not change. We  
 577 choose seven days assuming policy changes take a week to become effective and that  
 578 reasonable parameters can be expected to change within this time period. Also, the seven  
 579 day window size accounts for the fact that often data is not reported as diligently over the  
 580 weekend. Time series of the values of the parameters for the geographic locations  
 581 discussed in this paper can be found in the supplemental materials for Figure 2.

582 Given the restrictions on data available for the populations of various states,  
 583 varying all of the parameters results in an over parameterized system. Therefore, a subset  
 584 of the model parameters are fit while the others are either extracted from other sources;  
 585 see Table 5.

586

587



588 **Table 5.** Details of parameter values used for *SIDHRE-Q* Model.

Parameter	Details & Statistics			
$\alpha$	$\alpha$ is the probability that an interaction between an undetected infected person and an uninfected person results in a new infection, divided by the average number of uninfected people an undetected infected person comes into contact with on a given day. $\alpha$ is estimated from the data.		Mean	St. Dev.
		MA	0.088	0.051
		LA	0.090	0.034
		NYC	0.067	0.042
		SJRP	0.121	0.042
$\eta$	<p><math>\eta</math> is the probability that an interaction between an infected person and an uninfected person results in a new infection, divided by the average number of uninfected people a detected infected person comes into contact with on a given day. <math>\eta = 0.01 \cdot \alpha</math></p> <p>The constant relating <math>\eta, \alpha</math> accounts for a small but nonzero transmission due to the quarantined (detected) infected population. This value was chosen to be small, assuming a quarantined individual will only infect others with low probability.</p>			
$\nu$	$\nu$ is the probability that a symptomatic undetected individual is diagnosed on a given day. $\nu$ is estimated from the data. $\nu$ is multiplied by sensitivity (assume benchmark sensitivity 100% for PCR, as used when fitting).		Mean	St. Dev.
		MA	0.006	0.005
		LA	0.011	0.006
		NYC	0.0056	0.002
		SJRP	0.015	0.007
$\epsilon$	<p><math>\epsilon</math> is the probability that an asymptomatic undetected infected individual is diagnosed on a given day. <math>\epsilon = 0</math> while fitting (during PCR symptomatic testing). <math>\epsilon = (\text{sensitivity}/\text{days between tests})</math> when the rapid testing strategy is activated.</p>			
$\lambda$	<p><math>\lambda</math> is the probability that an undetected infected individual transitions to the recovered state on a given day. <math>\lambda = 1/14</math>, or the inverse of average recovery time.<sup>48</sup></p>			
$\mu$	$\mu$ is the probability that an infected individual develops severe symptoms on a given day and transitions into the hospitalized state. The flow from $D$ to $H$ is assumed to be independent of the ratio $I/D$ , but comes only from the detected infected population, hence why it is multiplied by $(I + D)/D$ . $\mu$ is estimated from the data.		Mean	St. Dev.
		MA	0.0013	9.5e-4
		LA	0.0016	2.4e-4
		NYC	0.0011	6.6e-4
		SJRP	0.0018	8.0e-4
$\rho$	<p><math>\rho</math> is the probability that a detected infected individual transitions to the recovered state on a given day.</p> <p><math>\rho = 1/14</math>, or the inverse of the average recovery time.<sup>48</sup></p>			

$\sigma$	$\sigma$ is the probability that a hospitalized individual transitions to the recovered state on a given day. $\sigma = 1/11$ , or the inverse of the average recovery time for a hospitalized individual. <sup>48</sup>			
$\tau$	$\tau$ is the probability that a hospitalized individual expires on a given day. $\tau$ is estimated from the data.		Mean	St. Dev.
		MA	0.034	0.012
		LA	0.016	0.004
		NYC	0.036	0.034
		SJRP	0.032	0.045
$\gamma$	$\gamma$ is the probability of entering either of the quarantine states on a given day from either the Susceptible or Recovered populations. $\gamma = 0$ while fitting (during PCR symptomatic testing). $\gamma = (1 - \text{specificity}) \times (1/\text{days between tests})$ when the rapid testing strategy is activated.			
$\psi$	$\psi$ is the probability that an individual exits quarantine on a given day. $\psi = 1/14$ , or the inverse of the quarantine period for fixed length quarantine.			

589

590 The fitting procedure minimizes the sum of the squared residuals of the total cases,  
 591 current daily hospitalizations, cumulative deaths, and percentage of total infected  
 592 individuals currently hospitalized. The first three are present in the data sets while the  
 593 latter is derived from the estimates of the ratio between infected undetected to infected  
 594 detected individuals from the CDC Laboratory Seroprevalence Survey Data<sup>49</sup>. While this  
 595 ratio changes over time, the percentage of infected individuals developing severe  
 596 symptoms should remain roughly constant throughout the course of the epidemic in the  
 597 different locations studied.

598 We consider the data sets for outbreaks in MA, NYC, LA, and SJRP, Brazil<sup>42-47</sup>.  
 599 While each location has testing and fatality information dating back to January,  
 600 hospitalization data was not included until late March (for NYC and SJRP) and April (for  
 601 MA and LA). Hence we begin our fitting procedure and testing strategy on 1 April for  
 602 each of the data sets; by this point, the outbreak is advanced in NYC, substantial in MA,  
 603 non-negligible, but far from its peak, in LA, and in early stages in SJRP, Brazil. Starting

604 simulations at various stages of the outbreak allows one to see the difference in results  
605 between when a testing strategy is administered.

606 In order to determine the effectiveness of the county-based strategy when applied  
607 to the state of California, we also fit all of the counties in California with a population  
608 greater than 1.5% of that of the entire state and with greater than zero deaths. The results  
609 do not depend on these selections, but instead suggest a practical criteria to administer  
610 limited resources. The fitting is done starting 10 April for these counties, as at this point  
611 the outbreak is sufficiently well-documented in each to successfully model. For the  
612 county-level data we compute a seven day running average of each of the data sets to  
613 which we then fit in order to smooth out fluctuations in the data, likely due to reporting,  
614 which are more significant here than in the other data sets considered, as the county  
615 populations are smaller and hence discrepancies impact the smoothness of the data  
616 more. The fits for each of the counties can be found in the supplementary materials to  
617 Figure 5.

618 As one can see from Figure 2, these data sets are particularly not smooth, which  
619 indicates inefficiencies in reporting. Additionally, it is difficult to gauge their consistency  
620 within the dates provided or to compare between locations, as reporting mechanisms  
621 changed over time within the same locations. Despite this lack of consistency, our model  
622 and fitting mechanism was successful in reproducing the progress of the outbreak in each  
623 data set studied.

624 The authors confirm that the data supporting the findings of this study are available within  
625 the article and/or its supplementary materials; any other data will be made available upon  
626 request. Our code can be found on github:

627 [https://github.com/badeaa3/COVID19\\_Rapid\\_Testing](https://github.com/badeaa3/COVID19_Rapid_Testing). The code is written using python  
628 with the packages scipy, numpy, lmfit, matplotlib and plotly<sup>50–54</sup>.

629

## 630 **Acknowledgments**

631 We thank Professor Lee Gehrke for critical reading of the manuscript. The study is  
632 funded, in part, by a Bill and Melinda Gates Foundation Award (INV-017872) to E25Bio,  
633 Inc. EN is funded by Tufts University DISC Seed Grant. MLN is supported by a FAPESP  
634 grant (#2020/04836-0) and is a CNPq Research Fellow. AFV is supported by a FAPESP  
635 Fellow grant (#18/17647-0). GRFC is supported by a FAPESP Fellow grant (#20/07419-  
636 0). BHGAM is supported by a FAPESP Scholarship (#19/06572-2). The funders had no  
637 role in the design of the study; in the collection, analyses, or interpretation of data; in the  
638 writing of the manuscript, or in the decision to publish the results.

639

## 640 **Competing Interest**

641 BN, AB, AR, MB, NS, AG, IB, and BBH are employed by or affiliated with E25Bio  
642 Inc. ([www.e25bio.com](http://www.e25bio.com)), a company that develops diagnostics for epidemic viruses.

643

## 644 **References**

- 645 1. Coronavirus Disease (COVID-19) Situation Reports.  
646 <https://www.who.int/emergencies/diseases/novel-coronavirus-2019/situation-reports>.
- 647 2. Menkir, T. F. *et al.* Estimating the number of undetected COVID-19 cases exported  
648 internationally from all of China. *medRxiv* (2020) doi:10.1101/2020.03.23.20038331.
- 649 3. Ivorra, B., Ferrández, M. R., Vela-Pérez, M. & Ramos, A. M. Mathematical modeling of the  
650 spread of the coronavirus disease 2019 (COVID-19) taking into account the undetected

- 651 infections. The case of China. *Commun Nonlinear Sci Numer Simul* 105303 (2020)  
652 doi:10.1016/j.cnsns.2020.105303.
- 653 4. Salathé, M. *et al.* COVID-19 epidemic in Switzerland: on the importance of testing, contact  
654 tracing and isolation. *Swiss Med Wkly* **150**, w20225 (2020).
- 655 5. Lau, H. *et al.* Evaluating the massive underreporting and undertesting of COVID-19 cases in  
656 multiple global epicenters. *Pulmonology* (2020) doi:10.1016/j.pulmoe.2020.05.015.
- 657 6. Silverman, J. D., Hupert, N. & Washburne, A. D. Using influenza surveillance networks to  
658 estimate state-specific prevalence of SARS-CoV-2 in the United States. *Science Translational*  
659 *Medicine* (2020) doi:10.1126/scitranslmed.abc1126.
- 660 7. Böhning, D., Rocchetti, I., Maruotti, A. & Holling, H. Estimating the undetected infections in  
661 the Covid-19 outbreak by harnessing capture-recapture methods. *Int. J. Infect. Dis.* **97**, 197–  
662 201 (2020).
- 663 8. Baek, Y. H. *et al.* Development of a reverse transcription-loop-mediated isothermal  
664 amplification as a rapid early-detection method for novel SARS-CoV-2. *Emerg Microbes Infect*  
665 **9**, 998–1007 (2020).
- 666 9. Leo, L. Mylab gets commercial approval from ICMR for Covid-19 antigen rapid testing kit.  
667 *Livemint* [https://www.livemint.com/news/india/mylab-gets-commercial-approval-from-icmr-](https://www.livemint.com/news/india/mylab-gets-commercial-approval-from-icmr-for-covid-19-antigen-rapid-testing-kit-11595434040321.html)  
668 [for-covid-19-antigen-rapid-testing-kit-11595434040321.html](https://www.livemint.com/news/india/mylab-gets-commercial-approval-from-icmr-for-covid-19-antigen-rapid-testing-kit-11595434040321.html) (2020).
- 669 10. Dey, S. Coronavirus testing: Rapid antigen tests now make up nearly half of daily checks |  
670 India News - Times of India. *The Times of India*  
671 [https://timesofindia.indiatimes.com/india/rapid-antigen-tests-now-make-up-nearly-half-of-](https://timesofindia.indiatimes.com/india/rapid-antigen-tests-now-make-up-nearly-half-of-daily-checks/articleshow/77340459.cms)  
672 [daily-checks/articleshow/77340459.cms](https://timesofindia.indiatimes.com/india/rapid-antigen-tests-now-make-up-nearly-half-of-daily-checks/articleshow/77340459.cms).
- 673 11. Vogels, C. B. F. *et al.* Analytical sensitivity and efficiency comparisons of SARS-CoV-2 RT-  
674 qPCR primer-probe sets. *Nat Microbiol* (2020) doi:10.1038/s41564-020-0761-6.
- 675 12. Larremore, D. B. *et al.* Test sensitivity is secondary to frequency and turnaround time for  
676 COVID-19 surveillance. *medRxiv* (2020) doi:10.1101/2020.06.22.20136309.

- 677 13. Shen, Z. *et al.* Superspreading SARS events, Beijing, 2003. *Emerging Infect. Dis.* **10**, 256–  
678 260 (2004).
- 679 14. Peiris, J. S. M. *et al.* Clinical progression and viral load in a community outbreak of  
680 coronavirus-associated SARS pneumonia: a prospective study. *Lancet* **361**, 1767–1772  
681 (2003).
- 682 15. He, X. *et al.* Temporal dynamics in viral shedding and transmissibility of COVID-19. *Nat. Med.*  
683 **26**, 672–675 (2020).
- 684 16. Giordano, G. *et al.* Modelling the COVID-19 epidemic and implementation of population-wide  
685 interventions in Italy. *Nat. Med.* **26**, 855–860 (2020).
- 686 17. Choi, S. & Ki, M. Estimating the reproductive number and the outbreak size of COVID-19 in  
687 Korea. *Epidemiol Health* **42**, e2020011 (2020).
- 688 18. Wei, Y. Y. *et al.* [Fitting and forecasting the trend of COVID-19 by SEIR(+CAQ) dynamic  
689 model]. *Zhonghua Liu Xing Bing Xue Za Zhi* **41**, 470–475 (2020).
- 690 19. Yang, Z. *et al.* Modified SEIR and AI prediction of the epidemics trend of COVID-19 in China  
691 under public health interventions. *J Thorac Dis* **12**, 165–174 (2020).
- 692 20. Cao, S., Feng, P. & Shi, P. [Study on the epidemic development of COVID-19 in Hubei  
693 province by a modified SEIR model]. *Zhejiang Da Xue Xue Bao Yi Xue Ban* **49**, 178–184  
694 (2020).
- 695 21. Huang, R., Liu, M. & Ding, Y. Spatial-temporal distribution of COVID-19 in China and its  
696 prediction: A data-driven modeling analysis. *J Infect Dev Ctries* **14**, 246–253 (2020).
- 697 22. Godio, A., Pace, F. & Vergnano, A. SEIR Modeling of the Italian Epidemic of SARS-CoV-2  
698 Using Computational Swarm Intelligence. *Int J Environ Res Public Health* **17**, (2020).
- 699 23. Gatto, M. *et al.* Spread and dynamics of the COVID-19 epidemic in Italy: Effects of emergency  
700 containment measures. *Proc. Natl. Acad. Sci. U.S.A.* **117**, 10484–10491 (2020).
- 701 24. Hou, C. *et al.* The effectiveness of quarantine of Wuhan city against the Corona Virus Disease  
702 2019 (COVID-19): A well-mixed SEIR model analysis. *J. Med. Virol.* **92**, 841–848 (2020).

- 703 25. Zhou, T. *et al.* Preliminary prediction of the basic reproduction number of the Wuhan novel  
704 coronavirus 2019-nCoV. *J Evid Based Med* **13**, 3–7 (2020).
- 705 26. Reno, C. *et al.* Forecasting COVID-19-Associated Hospitalizations under Different Levels of  
706 Social Distancing in Lombardy and Emilia-Romagna, Northern Italy: Results from an  
707 Extended SEIR Compartmental Model. *J Clin Med* **9**, (2020).
- 708 27. Alizargar, J. Risk of reactivation or reinfection of novel coronavirus (COVID-19). *J. Formos.*  
709 *Med. Assoc.* **119**, 1123 (2020).
- 710 28. Batisse, D. *et al.* Clinical recurrences of COVID-19 symptoms after recovery: viral relapse,  
711 reinfection or inflammatory rebound? *J. Infect.* (2020) doi:10.1016/j.jinf.2020.06.073.
- 712 29. Deng, W. *et al.* Primary exposure to SARS-CoV-2 protects against reinfection in rhesus  
713 macaques. *Science* (2020) doi:10.1126/science.abc5343.
- 714 30. Ota, M. Will we see protection or reinfection in COVID-19? *Nat. Rev. Immunol.* **20**, 351 (2020).
- 715 31. Victor Okhue, A. Estimation of the Probability of Reinfection With COVID-19 by the  
716 Susceptible-Exposed-Infectious-Removed-Undetectable-Susceptible Model. *JMIR Public*  
717 *Health Surveill* **6**, e19097 (2020).
- 718 32. Gu, Y. COVID-19 Projections Using Machine Learning. *COVID-19 Projections Using Machine*  
719 *Learning* <https://covid19-projections.com/>.
- 720 33. Stadlbauer, D. *et al.* Seroconversion of a city: Longitudinal monitoring of SARS-CoV-2  
721 seroprevalence in New York City. *medRxiv* 2020.06.28.20142190 (2020)  
722 doi:10.1101/2020.06.28.20142190.
- 723 34. Goodnough, A. & Shear, M. D. The U.S.'s Slow Start to Coronavirus Testing: A Timeline. *The*  
724 *New York Times* (2020).
- 725 35. Shear, M. D. *et al.* The Lost Month: How a Failure to Test Blinded the U.S. to Covid-19. *The*  
726 *New York Times* (2020).
- 727 36. Kaplan, S. & Thomas, K. Despite Promises, Testing Delays Leave Americans 'Flying Blind'.  
728 *The New York Times* (2020).

- 729 37. de Souza, W. M. *et al.* Epidemiological and clinical characteristics of the COVID-19 epidemic  
730 in Brazil. *Nature Human Behaviour* **4**, 856–865 (2020).
- 731 38. Mervosh, S. & Fernandez, M. ‘It’s Like Having No Testing’: Coronavirus Test Results Are Still  
732 Delayed. *The New York Times* (2020).
- 733 39. Gostic, K., Gomez, A. C., Mummah, R. O., Kucharski, A. J. & Lloyd-Smith, J. O. Estimated  
734 effectiveness of symptom and risk screening to prevent the spread of COVID-19. *eLife* **9**,  
735 e55570 (2020).
- 736 40. Zitek, T. The Appropriate Use of Testing for COVID-19. *West J Emerg Med* **21**, 470–472  
737 (2020).
- 738 41. Bosch, I. *et al.* Rapid antigen tests for dengue virus serotypes and Zika virus in patient serum.  
739 *Sci Transl Med* **9**, (2017).
- 740 42. Massachusetts Department of Public Health. COVID-19 Response Reporting. *Mass.gov*  
741 <https://www.mass.gov/info-details/covid-19-response-reporting>.
- 742 43. California Department of Public Health. COVID-19 Cases - California Open Data.  
743 <https://data.ca.gov/dataset/covid-19-cases>.
- 744 44. California Department of Public Health. COVID-19 Hospital Data - California Open Data.  
745 <https://data.ca.gov/dataset/covid-19-hospital-data>.
- 746 45. Department of Health and Human Hygiene. COVID-19 Daily Counts of Cases,  
747 Hospitalizations, and Deaths | NYC Open Data. <https://data.cityofnewyork.us/Health/COVID-19-Daily-Counts-of-Cases-Hospitalizations-and-Deaths/rc75-m7u3>.
- 749 46. Sao Jose do Rio Preto Public Health Office. *COVID-19 Surveillance Data, Sao Jose do Rio*  
750 *Preto*.
- 751 47. New York State Government. Daily Hospitalization Summary by Region. *New York Forward*  
752 <https://forward.ny.gov/daily-hospitalization-summary-region>.
- 753 48. Massachusetts General Hospital Institute for Technology Assessment. COVID-19 Simulator  
754 - Methodology. <https://www.covid19sim.org/images/docs/COVID->



- 755        19\_simulator\_methodology\_download\_20200507.pdf.
- 756    49. CDC. Coronavirus Disease 2019 (COVID-19). *Centers for Disease Control and Prevention*
- 757        <https://www.cdc.gov/coronavirus/2019-ncov/cases-updates/commercial-lab-surveys.html>
- 758        (2020).
- 759    50. SciPy.org — SciPy.org. <https://www.scipy.org/>.
- 760    51. NumPy. <https://numpy.org/>.
- 761    52. Non-Linear Least-Squares Minimization and Curve-Fitting for Python — Non-Linear Least-
- 762        Squares Minimization and Curve-Fitting for Python. <https://lmfit.github.io/lmfit-py/>.
- 763    53. Matplotlib: Python plotting — Matplotlib 3.3.1 documentation. <https://matplotlib.org/>.
- 764    54. Plotly: The front-end for ML and data science models. <https://plotly.com/>.